Egypt. J. Chem. **Vol. 66**, No. 8. pp. 467 - 483 (2023)

Egyptian Journal of Chemistry

http://ejchem.journals.ekb.eg/

Facile Synthesis, Inhibition of VEGFR-2, Anticancer activity, Molecular Dynamics Simulation And Target Identification Of Some New Pyrano thiazine derivatives

Walaa Salah Elserwy[1,*]; Neama Mohammed[1]; Weam Salah Elserwy[2]; Mohamed Abdalla[3], Ahmed El-Rashedy[2]

[1]*Department of Therapeutic Chemistry, Pharmaceutical and Drug Industries Research Institute, National Research Centre, Dokki, Cairo, Egypt, 12622.*

[2]*Department Of Microbial and Natural Products chemistry, Pharmaceutical and Drug Industries Research Institute, National Research Centre, Dokki, Cairo, Egypt, 12622.*

[3]*Atos Pharma, Elkatyba Land, Belbis, ElSharkya 44621, Egypt.*

Abstract

A new series of)2-amino-4-(substituted)-4,10-dihydrobenzo[b]pyrano[2,3-e][1,4]thiazine-3-carbonitrile(3(a, b) was synthesized by the reaction of 2-(substituted) malononitrile with 2H-benzo[b][1,4]thiazin-3(4H)-one as a key starting material,)2-amino-4-(substituted)-4,10-dihydrobenzo[b]pyrano[2,3-e][1,4]thiazine-3-carbonitrile(3(a, b) reacted with some reagents, namely, formic acid, sulphuric acid, thiosemicarbazide, ethyl acetoacetate, triethyl orthoformate, carbon disulphide, diethylmalonate, malononitrile, phosphoryl chloride , and acetic anhydride to produce compounds 4(a,b), 5(a,b), 6(a,b), 8(a,b), 9(a,b), 10(a,b),11(a,b),14(a,b),15(a,b), and 18(a,b) some of newly synthesized compounds were studied and screened for their in vitro anticancer activity. Moreover, molecular dynamics simulation and target identification studies were conducted to support the findings .All the newly synthesized compounds were structurally confirmed by various modern analytical methods (IR, 1H NMR and MS).

Keywords: *pyrano thiazine. VEGFR-2 ,Anticancer, molecular dynamics simulation.*

1. Introduction

New heterocyclic compounds have been a topic of great interest in the last few decades. This is because it has a wide range of applications. Heterocycles are essential to life and are very common in nature. Due to their pharmacological activity, 4H-pyran and its derivatives are of great interest[1] because they possess antispasmodic, anticoagulant, diuretic, anticancer, and antianaphylactic activities[2-4]. In addition, (4H-pyran) determine as a useful intermediate for synthesizing of various compounds such as pyranopyridine derivatives[5], polyazanaphthalenes [6] , pyranopyrimidines [7] , and pyridin-2-ones[8] . . Cancer is considered to be the leading cause of death in economically developed countries and is due to abnormal cell proliferation [9, 10] . In addition, protein kinases are involved in most signaling pathways leading to cancer cell proliferation and angiogenesis, including solid tumor growth. Colon, breast, gastric, and prostate cancers [11-13] . VEGFR-2 (Vascular Endothelial Growth Factor Receptor 2) is a receptor tyrosine kinase[14] , and its activation contributes may lead to increased tumor oxygenation [15, 16] . VEGFR-2 is most highly expressed in many cancers such as breast, hepatocellular and renal carcinomas [17-19] . As a result, inhibition of the VEGFR-2 signaling pathway is a very important property for anti-tumor therapy[20] . In this study, we investigated the anticancer activity of six synthetic compounds 3a, 4(a,b), 9(a,b), 18b against different human cancer cell lines.

*Corresponding author e-mail: awab_13@yahoo.com.; (Weam Salah Elserwy).
Received date 09 November 2022; revised date 05 December 2022; accepted date 08 December 2022
DOI: 10.21608/ejchem.2022.173057.7167

2. Experimental Section

2.1. Chemistry

All melting points are uncorrected and were taken in open capillary tubes using Electrothermal apparatus 9100. Elemental microanalyses were carried out at Microanalytical Unit, Central Services Laboratory, National Research Centre, Dokki, Cairo, Egypt, using VarioElementar and were found within ±0.4% of the theoretical values. Infrared spectra were recorded on FT/IR- 4100 Jasco-Japan, Fourier transform, Infrared spectrometer at cm-1 scale using KBr disc technique at Central Services Laboratory, National Research Centre, Dokki, Cairo, Egypt. 1H NMR and ^{13}C NMR spectra were determined by using a JEOL AS-500 NMR spectrometer at Central Services Laboratory, National Research Centre, Dokki, Cairo, Egypt. Varian Gemini200-Oxford 300 MHz and Merury Plus-Oxford 400 MHz at Ministry of defense, Chemical Warfare Department, The Main Chemical Warfare Laboratories, Cairo, Egypt. Chemical shifts were expressed in δ (ppm) downfield from tetramethylsilane as an internal standard. The mass spectra were measured with a GC MSQp1000EX Shimadzu, Cairo University, Cairo, Egypt, and with a Finnigan MAT SSQ-7000 mass spectrometer at Central Services Laboratory, National Research Centre, Dokki, Cairo, Egypt. Follow up of the reactions and checking the purity of the compounds were made by thin layer chromatography on silica gel-precoated aluminium sheets (Type 60, F 254, Merck, Darmstadt, Germany) using chloroform/methanol (20:2, v/v), and the spots were detected by exposure to UV lamp at λ254 nanometer for few seconds and by iodine vapor.

2.1.1. 2-amino-4-(substituted)-4,10 dihydrobenzo [b] pyrano [2,3-e] [1,4] thiazine-3-arbonitrile 3(a, b)

(0.01 mol) of **arylidenemalononitrles 1a,b** and benzothiazine 2 (0.01 mol) in methanol (25 ml) containing piperidine (3 ml) was refluxed for 8 h. After cooling the reaction mixture was filtered, dried and recrystallized [21].

2.1.2. 2-amino-4-(4-hydroxy-3-methoxyphenyl)-4,10-dihydrobenzo [b] pyrano [2,3-e] [1,4]thiazine-3-carbonitrile (3a)

Yield: 80%; M.p. 120-122°C. IR spectrum (KBr, ν, cm-1): 3415, 3317, 3191 (NH_2 & NH), 3019 (CH aromatic), 2219 (C≡N), 1679 (C=N), 1158 (C=S). ^{1}H-NMR (300 MHz, DMSO-d_6): 10.53 (s, 1H, D_2O-exchangeable, NH), 9.77 (s, 1H, D_2O-exchangeable, OH), 7.49-7.19 ((m, 7H, Ar-H),), 6.91 (s, 2H, D_2O-exchangeable, NH_2), 3.93 (s, 1H, CH of pyran),3.73(s, 3H, CH_3), .MS: m/z = 365.41. Anal. Calcd. For $C_{19}H_{15}N_3O_3S$ (365.41): C, 62.45; H, 4.14; N, 11.50; S, 8.77; found: C, 62.74; H, 4.02; N, 11.32; S, 8.90.

2.1.3. 2-amino-4-(3-methoxyphenyl)-4,10-dihydrobenzo[b]pyrano[2,3-e][1,4]thiazine-3-carbonitrile (3b)

Yield: 80%; M.p. 210-213°C. IR spectrum (KBr, ν, cm-1): 3419, 3342, 3199 (NH_2 & NH), 3062 (CH aromatic), 2214 (C≡N), 1661 (C=N), 1155 (C=S). ^{1}H-NMR (300 MHz, DMSO-d_6): 10.72 (s, 1H, D_2O-exchangeable, NH), 7.51-7.23 (m, 8H, Ar-H), 6.97 (s, 2H, D_2O-exchangeable, NH_2), 3.96 (s, 1H, CH of pyran),3.92(s, 3H, CH_3),. MS: m/z = 349.41. Anal. Calcd. For $C_{19}H_{15}N_3O_2S$ (349): C, 65.31; H, 4.33; N, 12.03; S, 9.18; found: C, 65.51; H, 4.59; N, 11.82; S, 9.31

2.1.4. 4-(substituted)-4, 10-dihydrobenzo [b] pyrano [2,3-e] [1,4] thiazin-2(3H)-one 4(a,b)

A mixture of 3a,b (0.01 mol), in formic acid (20 ml) was refluxed for 27 h. Left to cool, then collect the crude solid product that precipitated out by filtration by suction and recrystallized to afford 4a,b [21].

2.1.5. 4-(4-hydroxy-3-methoxyphenyl)-4,10-dihydrobenzo[b]pyrano[2,3-e] [1,4] thiazin-2(3H)-one [4a] :

3190 (NH), 3107 (CH aromatic), 2978 (CH aliphatic), 1676(C=O), 1196 (C=S).^{1}H-NMR (300 MHz, DMSO-d_6): 10.45 (s, 1H, D_2O-exchangeable, NH), 9.87 (s, 1H, D_2O-exchangeable, OH), 7.34-7.11 (m, 7H, Ar-H), 3.98(s, 1H, CH of pyran),3.77(s, 3H, CH_3), 2.53(s, 2H, CH_2).MS: m/z = 341.38. Anal. Calcd. For $C_{18}H_{15}NO_4S$ (341): C, 63.33; H, 4.43; N, 4.10; S, 9.39; found: C, 63.56; H, 4.20; N, 4.32; S, 9.51.

2.1.6. 4-(3-methoxyphenyl)-4,10-dihydrobenzo [b] pyrano[2,3-e] [1,4]thiazin-2(3H)-one (4b)

Yield: 70%; M.p. 145-146°C. IR spectrum (KBr, ν, cm-1): 3117 (NH), 3100 (CH aromatic), 295 (CH aliphatic), 1663(C=O), 1159 (C=S),) ^{1}H-NMR (300 MHz, DMSO-d_6): 10.74 (s, 1H, D_2O-exchangeable, NH), 7.52-7.21 ((m, 8H, Ar-H),), 3.97 (s, 1H, CH of pyran), 3.93(s, 3H, CH_3), 2.62(s, 2H, CH_2)**.** MS: m/z = 325.38. Anal. Calcd. For $C_{18}H_{15}NO_3S$ (325): C, 66.44; H, 4.65; N, 4.30; S, 9.85; found: C, 66.21; H, 4.72; N, 4.11; S, 10.01

2.1.7. 2-amino-4-(substituted)-4,10-dihydrobenzo[b]pyrano[2,3-e][1,4]thiazine-3-carboxylic acid 5(a,b)

A mixture of 3a,b (0.01 mol), in concentrated sulphuric acid (20 ml) below 5 °C and kept for 48 h at room temperature. The content was poured into ice cold water and filtered. The product was isolated and recrystallized to afford **5a, b** [21].

2.1.8. 2-amino-4-(4-hydroxy-3-methoxyphenyl)-4,10-dihydrobenzo[b]pyrano[2,3-e][1,4]thiazine-3-carboxylic acid (5a)

Yield: 70%; M.p. 180-182°C. IR spectrum (KBr, ν, cm-1): 3430, 3353, 3310 (OH& NH_2& NH), 3160 (CH aromatic), 1713 (C=O acid),^{1}H-NMR (300 MHz, DMSO-d_6): 11.45 (s, 1H, D_2O-exchangeable, COOH), 10.22 (s, 1H, D_2O-exchangeable, NH), 9.76 (s, 1H, D_2O-exchangeable, OH), 7.44-7.21 ((m, 7H, Ar-H),), 6.71 (s, 2H, D_2O-exchangeable, NH_2), 3.96(s, 1H, CH of pyran),3.64(s, 3H, CH_3)..MS: m/z = 384.41. Anal. Calcd. For $C_{19}H_{16}N_2O_5S$ (384): C, 59.37; H, 4.20; N, 7.29S, 8.34; found: C, 59.54; H, 4.02; N, 7.00 S, 8.54

2.1.9. 2-amino-4-(4-hydroxy-3-methoxyphenyl)-4,10-dihydrobenzo[b]pyrano[2,3-e][1,4]thiazine-3-carboxylic acid (5b)

Yield: 70%; M.p. 159-161°C. IR spectrum (KBr, ν, cm-1): 3432, 3350, 3300 (OH& NH_2& NH), 3146 (CH aromatic), 1704 (C=O acid),. ^{1}H-NMR (300 MHz, DMSO-d_6): 11.52 (s, 1H, D_2O-exchangeable, COOH), 10.30 (s, 1H, D_2O-exchangeable, NH), 7.64-7.40 (m, 8H, Ar-H), 6.92 (s, 2H, D_2O-exchangeable, NH_2), 3.93 (s, 1H, CH of pyran),3.70(s, 3H, CH_3)..MS: m/z = 368.41. Anal. Calcd. For $C_{19}H_{16}N_2O_4S$ (368): C, 61.94; H, 4.38; N, 7.60; S, 8.70; found: C, 61.79; H, 4.51; N, 7.45; S, 8.54

2.1.10. 3,4-diamino-5-(substituted)-3,4,5,11tetrahydro benzo [b]pyrimido [5',4':5,6] pyrano[2,3-e][1,4]thiazine-2(1H)-thione 6(a,b)

In oil bath, A mixture of 3a,b (0.02 mol), and thiosemicarbazide (2 mmol, 0.19 g) was fused at 180–185 °C for 3 hours under dry conditions. The fused mixture was then heated in ethanol (15 ml) and the precipitate that formed after cooling was collected by filtration, dried and then recrystallized to give compounds 6a,b[22] **.**

2.1.11. 3,4-diamino-5-(4-hydroxy-3-methoxyphenyl)-3,4,5,11-tetrahydrobenzo[b]pyrimido[5',4':5,6]pyrano[2,3-e][1,4]thiazine-2(1H)-thione (6a)

Yield: 70%; M.p. 160-163°C. IR spectrum (KBr, ν, cm-1): 3442, 3334, 3195 (NH and NH_2), 2219 (C—N), 1632 (C—N); ^{1}H-NMR (300 MHz, DMSO-d_6): 11.19,10.52 (2s, 2H, D_2O-exchangeable, 2NH), 9.42 (s, 1H, D_2O-exchangeable, OH), 7.45-7.02 (m, 7H, Ar-H), 8.59 (s, 2H, D_2O-exchangeable, NH_2), 3.90(s, 1H, CH of pyran),3.64(s, 3H, CH_3) ,3.44 (s, 2H, D_2O-exchangeable, NH_2)..MS: m/z = 441.09. Anal. Calcd. For $C_{20}H_{19}N_5O_3S_2$ (441): C, 54.41; H, 4.34; N, 15.86; S, 14.52; found: C, 54.60; H, 4.18; N, 15.67; S, 14.72

2.1.12. 3,4-diamino-5-(3-methoxyphenyl)-3,4,5,11-tetrahydrobenzo[b]pyrimido[5',4':5,6]pyrano[2,3-e][1,4]thiazine-2(1H)-thione(6b)

Yield: 70%; M.p. 110-112°C. IR spectrum (KBr, ν, cm-1): 3434, 3322, 3175 (NH and NH_2), 2214 (C—N), 1634 (C—N); ^{1}H-NMR (300 MHz, DMSO-d_6): 11.32,10.72 (2s, 2H, D_2O-exchangeable, 2NH),, 7.55-7.32 (m, 8H, Ar-H), 8.71 (s, 1H, D_2O-exchangeable, NH_2), 3.74(s, 3H, CH_3) , 3.93(s, 1H, CH of pyran),3.49 (s, 1H, D_2O-exchangeable, NH_2)..MS: m/z = 425.53. Anal. Calcd. For $C_{20}H_{19}N_5O_2S_2$ (425): C, 56.45; H, 4.50; N, 16.46; S, 15.07; found: C, 56.30; H, 4.70; N, 16.23; S, 14.89

2.1.13. 1-(4-amino-2-hydroxy-5-(substituted)-3,4,5,11-tetrahydrobenzo[b]pyrido[3',2':5,6]pyrano[2,3-e][1,4]thiazin-3-yl)ethan-1-one 8(a,b)

A mixture of 3a,b (0.04 mol), ethyl acetoacetate (0.04 mol, 0.52 ml) and potassium carbonate (0.06 mol, 0.83 g) in 15 ml DMF heated under reflux for 12 hours. The reaction mixture allowed to cool at room temperature, and then poured into ice-cooled water followed by neutralized by drops of dilute HCl. The

solid product that obtained by filtration purified by recrystallization from EtOH to obtain 8a,b[22] **.**

2.1.14. 1-(4-amino-2-hydroxy-5-(4-hydroxy-3-methoxyphenyl)-3,4,5,11-tetrahydrobenzo[b]pyrido[3',2':5,6]pyrano[2,3-e][1,4]thiazin-3-yl)ethan-1-one(8a)

Yield: 70%; M.p. 170-172°C. IR spectrum (KBr, ν, cm-1): 3293, 3262, 3202 (NH_2 and OH), 2220 (C—N), 1712 (C—O), 1674 (C—N); ^{1}H-NMR (300 MHz, DMSO-d_6): 12.21,9.32 (2s, 2H, D_2O-exchangeable, 2OH), 10.52 (s, 1H, D_2O-exchangeable, NH), 7.31-7.14 ((m, 7H, Ar-H),), 6.93 (s, 2H, D_2O-exchangeable, NH_2), 3.97 (s, 1H, CH of pyran),3.44(s, 3H, CH_3).MS: m/z = 451.50. Anal. Calcd. For $C_{23}H_{21}N_3O_5S$ (451): C, 61.19; H, 4.69; N, 9.31; S, 7.10; found: C, 61.39; H, 4.80; N, 9.11; S, 7.33

2.1.15. 1-(4-amino-2-hydroxy-5-(3-methoxyphenyl)-3,4,5,11-tetrahydrobenzo[b]pyrido[3',2':5,6]pyrano[2,3-e][1,4]thiazin-3-yl)ethan-1-one(8b)

Yield: 70%; M.p. 117-110°C. IR spectrum (KBr, ν, cm-1):): 3283, 3231, 3199 (NH_2 and OH), 2211 (C—N), 1702 (C—O), 1664 (C—N);); ^{1}H-NMR (300 MHz, DMSO-d_6): 12.31 (s, 1H, D_2O-exchangeable, OH),10.62 (s, 1H, D_2O-exchangeable, NH), , 7.41-7.24 ((m, 8H, Ar-H),), 6.88 (s, 2H, D_2O-exchangeable, NH_2), 3.90 (s, 1H, CH of pyran),3.51(s, 3H, CH_3).MS: m/z = 435.50. Anal. Calcd. For $C_{23}H_{21}N_3O_4S$ (435): C, 63.43; H, 4.86; N, 9.65; S, 7.36; found: C, 63.59; H, 4.61; N, 9.57; S, 7.55

2.1.16. ethyl (Z)-N-(3-cyano-4-(substituted)-4,10-dihydrobenzo[b]pyrano[2,3-e][1,4]thiazin-2-yl)formimidate 9(a,b)

To a mixture of triethyl orthoformate (0.05 mol, 0.75 ml) and acetic anhydride (20 ml), 3a,b (0.05 mol), was added. The reaction mixture was refluxed for 5 hrs and the solvent was removed under reduced pressure. The separated solid was recrystallized to afford 9a,b[22] **.**

2.1.17. Ethyl (Z)-N-(3-cyano-4-(4-hydroxy-3-methoxyphenyl)-4,10-dihydrobenzo[b]pyrano[2,3-e][1,4]thiazin-2-yl)formimidate (9a)

Yield: 70%; M.p. 103-105°C. IR spectrum (KBr, ν, cm-1): 2233 (C—N), 1638 (C—N);); ^{1}H-NMR (300 MHz, DMSO-d_6): 10.52 (s, 1H, D_2O-exchangeable, NH), 9.82 (s, 1H, D_2O-exchangeable, OH), 7.72-7.14 ((m, 7H, Ar-H),), 4.01 (q, 2H, CH_2), 3.80 (s, 1H, CH of pyran),3.44(s, 3H, CH_3) 1.34 (t, 3H, CH_3). MS: m/z = 421.11 Anal. Calcd. For $C_{22}H_{19}N_3O_4S$ (421): C, 62.70; H, 4.54; N, 9.97; S, 7.61; found: C, 62.56; H, 4.32; N, 9.87; S, 7.87

2.1.18. ethyl (Z)-N-(3-cyano-4-(3-methoxyphenyl)-4,10-dihydrobenzo[b]pyrano[2,3-e][1,4]thiazin-2-yl)formimidate(9b)

Yield: 70%; M.p. 128-130°C. IR spectrum (KBr, ν, cm-1):): 2211 (C—N), 1623 (C—N).^{1}H-NMR (300 MHz, DMSO-d_6): 10.73 (s, 1H, D_2O-exchangeable, NH), 9.90 (s, 1H, D_2O-exchangeable, OH), 7.82-7.23 (m, 8H, Ar-H), 4.21 (q, 2H, CH_2), 3.90 (s, 1H, CH of pyran),3.54(s, 3H, CH_3) 1.42 (t, 3H, CH_3). MS: m/z = 405.11 Anal. Calcd. For $C_{22}H_{19}N_3O3S$ (405): C, 65.17; H, 4.72; N, 10.36; S, 7.91; found: C, 65.34; H, 4.87; N, 10.45; S, 8.12

2.1.19. 5-(substituted)-1,2,5,11-tetrahydrobenzo [b]pyrimido [5',4':5,6]pyrano[2,3-e][1,4]thiazine-2,4-dithiol 10(a,b)

To a solution of 3a,b (0.01 mol) in DMF (30 mL) or alcoholic KOH (5 gm/100 ml EtOH), CS2 (20 ml) was added dropwise. The reaction mixture was refluxed on a water-bath for 12 hr. The solvent was evaporated and mass obtained was triturated with water then crystallized to give 10a,b [23]**.**

2.1.20. 4-(2,4-dimercapto-1,2,5,11-tetrahydrobenzo[b]pyrimido[5',4':5,6]pyrano[2,3-e][1,4]thiazin-5-yl)-2-methoxyphenol (10a)

Yield: 70%; M.p. 180-183°C. IR spectrum (KBr, ν, cm-1): : 3311, 3196, 3062 (3 NH) 1380 (NCS), 1239, 1156 (C=S, C-S). ^{1}H-NMR (300 MHz, DMSO-d_6): 10.50,1.50(2s, 2H, D_2O-exchangeable, 2NH), 9.82 (s, 1H, D_2O-exchangeable, OH), 7.67-7.13 ((m, 7H, Ar-H),), 3.70 (s, 1H, CH of pyran),3.44(s, 3H, CH_3) 1.43,1.40 (2s, 2H, D_2O-exchangeable, 2SH).MS: m/z = 443.55, Anal. Calcd. For $C_{20}H_{17}N_3O_3S_3$ (443): C, 54.16; H, 3.86; N, 9.47; S, 21.68; found: C, 54.32; H, 3.59; N, 9.21; S, 21.90

2.1.21. 5-(3-methoxyphenyl)-1,2,5,11-tetrahydrobenzo[b]pyrimido[5',4':5,6]pyrano[2,3-e][1,4]thiazine-2,4-dithiol (10b)

Yield: 70%; M.p. 110-112°C. IR spectrum (KBr, ν, cm-1): 3305, 3170, 3085 (3 NH) 1361 (NCS), 1222, 1180 (C=S, C-S). 10.73,1.54(2s, 2H, D_2O-exchangeable, 2NH), 7.87-7.33 (m, 8H, Ar-H), 3.81 (s, 1H, CH of pyran),3.51(s, 3H, CH_3) 1.52,1.54 (2s, 2H, D_2O-exchangeable, 2SH).MS: m/z = 427.56Anal. Calcd. For $C_{20}H_{17}N_3O_2S_3$ (427): C, 56.18; H, 4.01; N, 9.83; S, 22.50; found: C, 56.35; H, 4.24; N, 9.98; S, 22.32

2.1.22. ethyl 4-amino-2-hydroxy-5-(substituted)-3,4,5,11-tetrahydrobenzo [b]pyrido [3',2':5,6]pyrano[2,3-e][1,4]thiazine-3-carboxylate 11(a,b)

A mixture of 3a,b (0.02 mol) and diethylmalonate (0.02 mol) was added to 20 mL freshly prepared sodium ethoxide solution [prepared by adding 1.0 g sodium metal into absolute ethanol (20 mL)] and the mixture was refluxed for 7 h, and left to cool overnight. The solid product so formed was collected by filtration, washed with ethanol and crystallized to give 11a,b [24]**.**

2.1.23. ethyl 4-amino-2-hydroxy-5-(4-hydroxy-3-methoxyphenyl)-3,4,5,11-tetrahydrobenzo [b]pyrido[3',2':5,6]pyrano[2,3-e][1,4]thiazine-3-carboxylate (11a)

Yield: 70%; M.p. <300°C. IR spectrum (KBr, ν, cm-1): 3423 and 3395 (NH_2), 3243 (br, OH), 1646 (C=O); ^{1}H-NMR (300 MHz, DMSO-d_6): 12.10,9.50(2s, 2H, D_2O-exchangeable, 2OH), 10.82 (s, 1H, D_2O-exchangeable, NH), 7.31-7.16 (m, 7H, Ar-H), 6.52 (s, 2H, D_2O-exchangeable, NH_2), 4.11 (q, 2H, CH_2), 4.01 (s, 1H, CH of pyran),3.51(s, 3H, CH_3) 1.57 (t, 3H, CH_3). .MS: m/z = 481.52Anal. Calcd. For $C_{24}H_{23}N_3O_6S$ (481): C, 59.87; H, 4.81; N, 8.73; S, 6.66; found: C, 59.65; H, 4.56; N, 8.54; S, 6.86

2.1.24. ethyl 4-amino-2-hydroxy-5-(3-methoxyphenyl)-3,4,5,11-tetrahydrobenzo [b]pyrido [3',2':5,6]pyrano[2,3-e][1,4]thiazine-3-carboxylate (11b)

Yield: 70%; M.p. 159-161°C. IR spectrum (KBr, ν, cm-1):): 3403 and 3375 (NH_2), 3229 (br, OH), 1623 (C=O); ^{1}H-NMR (300 MHz, DMSO-d_6): 12.23(s, H, D_2O-exchangeable, OH), 10.90 (s, 1H, D_2O-exchangeable, NH), 7.51-7.23 (m, 8H, Ar-H), 6.65 (s, 2H, D_2O-exchangeable, NH_2), 4.34 (q, 2H, CH_2), 4.11 (s, 1H, CH of pyran),3.63(s, 3H, CH_3) 1.57 (t, 3H, CH_3). MS: m/z = 465.52 Anal. Calcd. For $C_{24}H_{23}N_3O_5S$ (465): C, 61.92; H, 4.98; N, 9.03; S, 6.89; found: C, 62.11; H, 4.78; N, 9.32; S, 6.67

2.1.25. 5-(substituted)-5,11-dihydrobenzo[b]pyrimido[5',4':5,6]pyrano[2,3-e][1,4]thiazin-4-ol 14(a,b)

A mixture of 3a,b (0.02 mol) and phosphoryl chloride (3.83 g, 0.02 mol) in anhydrous DMF (5 mL) was heated under stirring at 70oC for 3 h. Then, the reaction mixture was poured onto ice and treated with aqueous ammonia (pH 8). A white solid separated and it was filtered off, washed with water, dried and recrystallized from an appropriate solvent to afford 14(a,b) [24]**.**

2.1.26. 5-(4-hydroxy-3-methoxyphenyl)-5,11-dihydrobenzo[b]pyrimido [5',4':5,6]pyrano[2,3-e][1,4]thiazin-4-ol (14a)

Yield: 70%; M.p. 205-207°C. IR spectrum (KBr, ν, cm-1): 3245 (br,OH). ^{1}H-NMR (300 MHz, DMSO-d_6): 10.70 (s, 1H, D_2O-exchangeable, NH), 9.45(s, H, D_2O-exchangeable, OH), 7.51-7.20 ((m, 8H, Ar-H),),4.31 (s, 1H, CH of pyran),3.71(s, 3H, CH_3). MS: m/z = 393.42Anal. Calcd. For $C_{20}H_{15}N_3O_4S$ (393): C, 61.06; H, 3.84; N, 10.68; S, 8.15; found: C, 61.32; H, 3.65; N, 10.90; S, 8.02

2.1.27. 5-(3-methoxyphenyl)-5,11-dihydrobenzo[b]pyrimido [5',4':5,6] pyrano[2,3-e][1,4]thiazin-4-ol (14b)

Yield: 70%; M.p. 157-160°C. IR spectrum (KBr, ν, cm-1):): 3201 (br,OH). ^{1}H-NMR (300 MHz, DMSO-d_6): 10.81 (s, 1H, D_2O-exchangeable, NH), 7.51-7.20 (m, 9H, Ar-H),4.52 (s, 1H, CH of pyran),3.78(s, 3H, CH_3). MS: m/z = 377.42. Anal. Calcd. For $C_{20}H_{15}N_3O_3S$ (477): C, 63.65; H, 4.01; N, 11.13; S, 8.49; found: C, 63.83; H, 4.32; N, 11.45; S, 8.19

2.1.28. 3-acetyl-5-(substituted)-2-methyl-5,11-dihydrobenzo[b] pyrimido [5',4':5,6]pyrano[2,3-e][1,4]thiazin-4(3H)-one 15(a,b)

A solution of 3a,b (0.01 mol) in acetic anhydride (20 ml) was heated under reflux for (10 min). The reaction mixture was concentrated. The solid crystallized to give 15a,b **[25].**

2.1.29. 3-acetyl-5-(4-hydroxy-3-methoxyphenyl)-2-methyl-5,11-

dihydrobenzo[b]pyrimido [5',4':5,6]pyrano[2,3-e][1,4]thiazin-4(3H)-one (15a)

Yield: 70%; M.p. 178-180°C. IR spectrum (KBr, ν, cm-1): 3310 (NH), 3062 (CH arom.), 2976, 2910 (CH-aliph.), 2209 (C:N), 1696 (C=O), ^{1}H-NMR (300 MHz, DMSO-d_6): 10.52 (s, 1H, D_2O-exchangeable, NH), 9.45(s, 1H, D_2O-exchangeable, OH), 7.32-7.14 (m, 7H, Ar-H),4.21 (s, 1H, CH of pyran),3.41,3.32(2s, 6H, $2CH_3$). MS: m/z = 449.48 Anal. Calcd. For $C_{23}H_{19}N_3O_5S$ (449): C, 61.46; H, 4.26; N, 9.35; S, 7.13; found: C, 61.76; H, 4.43; N, 9.65; S, 7.01

2.1.30. 3-acetyl-5-(3-methoxyphenyl)-2-methyl-5,11-dihydrobenzo[b]pyrimido[5',4':5,6]pyrano[2,3-e][1,4]thiazin-4(3H)-one (15b)

Yield: 70%; M.p. 142-145°C. IR spectrum (KBr, ν, cm-1): 3301 (NH), 3034 (CHarom.), 2942, 2903 (CH-aliph.), 22001 (C:N), 1673 (C=O), ^{1}H-NMR (300 MHz, DMSO-d_6): 10.70 (s, 1H, D_2O-exchangeable, NH), 7.54-7.23 (m, 8H, Ar-H),4.34 (s, 1H, CH of pyran),3.51,3.40(2s, 6H, $2CH_3$). MS: m/z = 433.11Anal. Calcd. For $C_{23}H_{19}N_3O_4S$ (433): C, 63.73; H, 4.42; N, 9.69; S, 7.40; found: C, 63.97; H, 4.56; N, 9.46; S, 7.63.

2.1.31. N-(3-cyano-4-(substituted)-4, 10-dihydrobenzo[b]pyrano[2,3-e][1,4]thiazin-2-yl)acetamide 18(a,b)

A solution of of 3a,b (0.01 mol) in acetic anhydride (20 ml) was heated under reflux for 10 hours and the reaction mixture was then concentrated. The solid crystallized to give 18a,b [25]**.**

2.1.32. N-(3-cyano-4-(4-hydroxy-3-methoxyphenyl)-4,10-dihydrobenzo[b]pyrano[2,3-e][1,4]thiazin-2-yl)acetamide (18a)

Yield: 70%; M.p. 113-115°C. IR spectrum (KBr, ν, cm-1): 3395 (NH), 3100 (CH-arom.), 2966, 2935 (CH-aliph.), 1712, 1687 (2C=O), 1558 (C=N).^{1}H-NMR (300 MHz, DMSO-d_6): 10.52,8.41 (2s, 2H, D_2O-exchangeable, 2NH), 9.85(s, H, D_2O-exchangeable, OH), 7.72-7.16 (m, 7H, Ar-H),4.11 (s, 1H, CH of pyran),3.66,1.86(2s, 6H, $2CH_3$).. MS: m/z = 407.44 Anal. Calcd. For $C_{21}H_{17}N_3O_4S$ (407): C, 61.91; H, 4.21; N, 10.31; S, 7.87; found: C, 61.79; H, 4.45; N, 10.52; S, 7.68

2.1.33. N-(3-cyano-4-(3-methoxyphenyl)-4, 10-dihydrobenzo[b]pyrano[2,3-e][1,4]thiazin-2-yl)acetamide (18b)

Yield: 70%; M.p. 98-101°C. IR spectrum (KBr, ν, cm-1): 3376 (NH), 3987 (CH-arom.), 2945, 2911 (CH-aliph.), 1702, 1654 (2C=O), 1523 (C=N), ^{1}H-NMR (300 MHz, DMSO-d_6): 10.72,9.23 (2s, 2H, D_2O-exchangeable, 2NH), 7.90-7.32 (m, 7H, Ar-H),4.31 (s, 1H, CH of pyran),3.82,1.90(2s, 6H, $2CH_3$).. MS: m/z = 391.45 Anal. Calcd. For $C_{21}H_{17}N_3O_3S$ (391): C, 64.44; H, 4.38; N, 10.73; S, 8.19; found: C, 64.71; H, 4.51; N, 10.54; S, 8.27

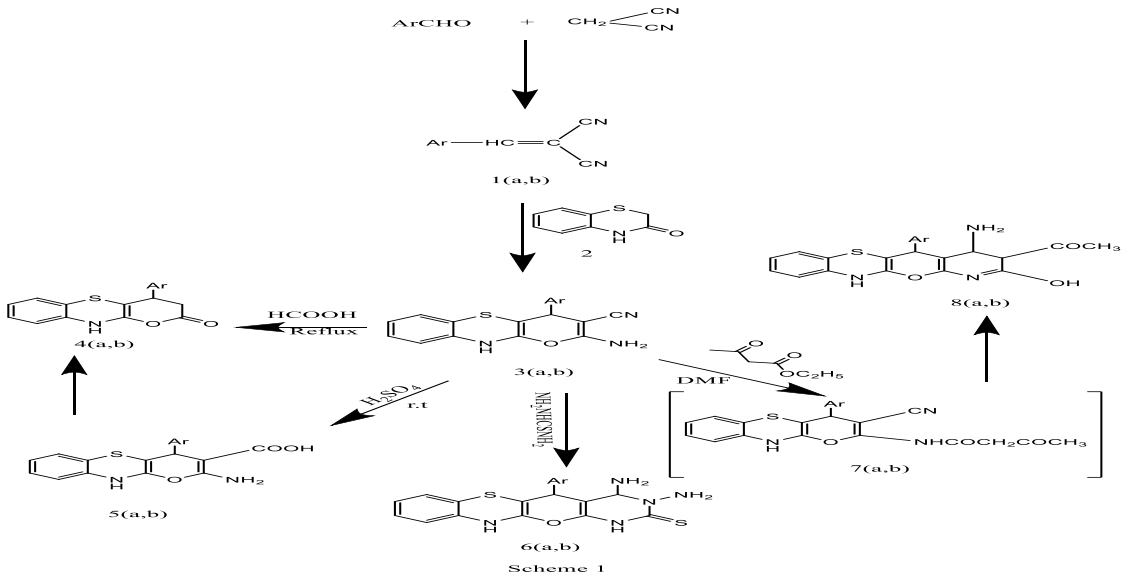

Scheme 1

*2.2. Biology***:**

2.2.1. Kinase assay

Via radiometric assay Inhibition of CDKs was evaluated using the Millipore Kinase Profiler services. Half-maximal inhibition (IC_{50}) values were calculated from 10-point dose–response curves and apparent inhibition constants (Ki) were calculated from the IC_{50} values and appropriate km (ATP) values for the kinases in question

2.2.1.1. VEGFR-2 kinase activity assays by ELISA

As a substrate, the assay performed in 96-well plates pre-coated with 20 μg ml−1 poly (Glu, Tyr) 4 : 1. In each well, 85 μl of an 8 μM ATP solution and 10 μl of the compounds added at varying concentration. Using Sorafenib as a positive control, and 0.1% (v/v) DMSO was the negative control. Experiments at each concentrations were performed in triplicate. The reaction initiated by adding 5 μl of VEGFR-2 kinase. After incubation for 1 h at 37 °C, the plate washed 3 times with PBS containing 0.1% Tween 20 (T-PBS). Next, 100 μl of anti-phosphotyrosine (PY99; 1 : 500 dilution) antibody was added. After 1 h of incubation at room temperature, the plate washed 3times. Goat anti-mouse IgG horseradish peroxidase (100 μl; 1 : 2000 dilution) diluted in T-PBS containing 5 mg ml−1 BSA was added. The plate Re-incubation at room temperature for 1 hour, and washed as before. At the end, 100 μl of developing solution (0.03% H_2O_2, 2 mg ml−1o-phenylenediamine in citrate buffer 0.1 M, pH 5.5) added and incubated at room temperature until color emerged. The reaction was terminated by the addition of 100 μl of 2 M H_2SO_4, and A_{492} was measured using a multiwell spectrophotometer (VERSAmax™) [26].

The inhibition rate (%) was calculated using the equation:

Inhibition rate (%) = [1 − (A_{492}/A_{492} control)] × 100%.

2.2.2. MTT toxicity assays

The cytotoxicity of the newly synthesized compounds against cancer cell lines in vitro performed with the MTT assay according to the Mosmann's method. The MTT assay is based on the reduction of the soluble 3-(4,5-methyl-2-thiazolyl)-2,5-diphenyl-2H-tetrazolium bromide (MTT) into a blue-purple formazan product, mainly by mitochondrial reductase activity inside living cells.

The cells used in cytotoxicity assay were cultured in RPMI 1640 medium supplemented with 10% fetal calf serum. Cells suspended in the medium (2 X 10^4 mL) were plated in 96-well culture plates and incubated at 37 °C in a 5% CO_2 incubator. After 12 hours, the test sample (2 μL) was added to the cells (2 X 10^4) in 96-well plates and cultured at 37 °C for 3 days. The cultured cells were mixed with 20 μL of MTT solution and incubated for 4 hours at 37 °C.crystals which were formed by the cellular reduction of MTT. After mixing with a mechanical plate mixer, the absorbance of each well was measured by a microplate reader using a test wavelength of 570 nm.

The results were expressed as the IC_{50}, which induced a 50% inhibition of treated cell growth when compared to the growth of control cells. Each experiment was performed at least 3 times.

There was a good reproducibility between replicate wells with standard errors below 10%.

2.3. Molecular dynamics simulation and target identification

2.3.1. System preparation

The crystal structure of the human CDK-activating kinase (CAK) ,and Vascular endothelial growth factor receptor 2 (VEGFR2s) were retrieved from the protein data bank with codes6XD3,and 4ASD, respectively [27, 28]. These compounds were then prepared for the molecular dynamics (MD) studies by using UCSF Chimera [29]. Using PROPKA, pH was fixed and optimized to 7.5[30]. Compound (14b) was drawn by ChemBioDraw Ultra 12.1[31]. Altogether, as described in the simulation section, the two prepared systems were subjected to 20 ns MD simulations.

2.3.1.1. Molecular dynamics (MD) simulations

Integration of Molecular dynamics (MD) simulations in biological systems' study enable exploring the physical motion of molecules and atoms that cannot be easily accessed by any other means[32].The insight extracted from performing this simulation provides an intricate perspective into the biological systems' dynamical evolution, such as conformational changes and molecule association [32] .The Molecular dynamics (MD) simulations of all systems were performed by using the GPU version of

the PMEMD engine present in the AMBER 18 package[33].

The partial atomic charge of each compound calculated with ANTECHAMBER's General Amber Force Field (GAFF) technique[34]. The Leap module of the AMBER 18 package implicitly solvated each system within an orthorhombic box of TIP3P water molecules within 10 Å of any box edge. The Leap module was used to neutralize each system by incorporating Na+ and Cl- counter ions. A 2000-step initial minimization of each system was carried out in the presence of a 500 kcal/mol applied restraint potential, followed by a 1000-step full minimization using the conjugate gradient algorithm without restraints.

During the Molecular dynamics (MD) simulation, each system was gradually heated from 0K to 300K over 500ps, ensuring that all systems had the same amount of atoms and volume. (The system's solutes were subjected to a 10kcal/mol potential harmonic constraint and a 1ps collision frequency). Following that, each system was heated and equilibrated for 500ps at a constant temperature of 300K.To simulate an isobaric-isothermal (NPT) ensemble, the number of atoms and pressure within each system for each production simulation were kept constant, the Berendsen barostat used with the system's pressure maintained at 1 bar [35].

For 20 ns, each system was Molecular dynamics (MD) simulated. The SHAKE method used to constrain the hydrogen bond atoms in each simulation. Each simulation used a 2fs step size and integrated an SPFP precision model. An isobaric-isothermal ensemble (NPT) with randomised seeding, constant pressure of 1 bar, a pressure-coupling constant of 2ps, a temperature of 300K, and a Langevin thermostat with a collision frequency of 1ps was used in the simulations.

2.3.1.2. Post-MD Analysis

After saving the trajectories obtained by Molecular dynamics (MD) simulations every 1 ps, the trajectories analyzed using the AMBER18 suite's CPPTRAJ [36] module. to create all graphs and visualizations ,The Origin [37] data analysis program and Chimera [29] were used.

2.3.1.3. Thermodynamic calculation

The Poisson-Boltzmann or generalized Born and surface area continuum solvation (MM/PBSA and MM/GBSA) approach has been found to be useful in estimation of ligand-binding affinities [38-40] . The Protein-Ligand complex molecular simulations used by MM/GBSA and MM/PBSA compute rigorous statistical-mechanical binding free energy within a defined force field.

Binding free energy averaged over 500 snapshots extracted from the entire 50 ns trajectory. The estimation of the change in binding free energy (ΔG) for each molecular species (complex, ligand, and receptor) can be represented as follows[41] :

$$\Delta G_{bind} = G_{complex} - G_{receptor} - G_{ligand} \quad (1)$$

$$\Delta G_{bind} = E_{gas} + G_{sol} - TS \quad (2)$$

$$E_{gas} = E_{int} + E_{vdw} + E_{ele} \quad (3)$$

$$G_{sol} = G_{GB} + G_{SA} \quad (4)$$

$$G_{SA} = \gamma SASA \quad (5)$$

The terms Egas, Eint, Eele, and Evdw symbolize the gas-phase energy, internal energy, Coulomb energy, and van der Waals energy. The Egas was directly assessed from the FF14SB force field terms. Solvation-free energy (Gsol) was evaluated from the energy involvement from the polar states (GGB) and non-polar states (G). The non-polar solvation free energy (GSA) was determined from the Solvent Accessible Surface Area (SASA)[42, 43] using a water probe radius of 1.4 Å. In contrast, solving the GB equation assessed the polar solvation (GGB) contribution. Items S and T symbolize the total entropy of the solute and temperature, respectively.

3. Results and discussion

3.1. Chemistry

(2-amino-4-(substituted)-4,10-dihydrobenzo[b]pyrano[2,3-e][1,4]thiazine-3-carbonitrile) 3(a, b) synthesized as the reported method [11] , formic acid and sulphoric acid reacted with compounds 3(a, b) to give compounds 4(a,b) and 5(a,b) respectively, according to the method [11].

(Scheme 1). ^{1}H NMR for compound 4(a,b) confirmed the proposed structure due to the appearance of (NH_2). Treatment of the compounds 3(a, b) with concentrated thiosemicarbazide led to the formation of compound 6(a,b) according to the method [12]. (Scheme 1). Significant indication for the formation of compounds 6(a,b) provided by IR bands, Heating of ethyl acetoacetate in dimethyl formamide with compound **3 (a,b)** in the presence of equimolar amount of potassium carbonate result in one spot on TLC, the result product was identified as 1-(4-amino-2-hydroxy-5-(substituted)-3,4,5,11-tetrahydrobenzo[b]pyrido [3',2':5,6]pyrano[2,3-e][1,4]thiazin-3-yl)ethan-1-one 8(a,b) according to the method [12]. (Scheme 1). The formation of ***8(a,b)*** was appeared to be proceeds via heterocyclization of the expected intermediate (N-(4-(substituted)3-cyano-4,10-dihydro benzo[b]pyrano[2,3-e] [1,4] thiazin-2-yl)-3-oxobutanamide) ***7(a,b)*** By Characteristic IR bands we proved the formation of compounds ***8(a,b)*** , compounds 3(a, b) When reacted with acetic anhydride in the presence of triethyl orthoformate , compounds 9(a,b) are formed according to method [12]. (Scheme 2). ^{1}H NMR for compound 9(a,b) confirmed the proposed structure due to the disappearance of (NH_2) and appearance of (CH_2CH_3) Also compound 10 (a,b) prepared by the reaction of compound 3(a,b) with CS_2 in the presence of alcoholic KOH in DMF according to the method [13]. (Scheme 2). ^{1}H NMR for compounds 10(a, b) confirmed the proposed structure due to the disappearance of (NH_2) group.

Treatment of 3(a,b) diethylmalonate and phosphoryl chloride in anhydrous DMF gave the corresponding derivatives 11(a,b) and 14(a,b) according to the method [14] . (Scheme 2). Confirmation of the synthesized compounds 11(a,b) and 14(a,b) was done using ^{1}H NMR spectroscopic data. For example disappearance of (NH_2) group.

When 3(a,b) briefly (10 min) refluxing with acetic anhydride gave the monoacetyl derivatives 15(a,b).; after reflux for a long time (10 h) the cyclic intermediate 5-(substituted-2-methyl-5,11-dihydro-4H-benzo[5',6'][1,4]thiazino[2',3':5,6]pyrano[2,3-d][1,3]oxazin-4-imine 16(a,b) was obtained, then rearrangement occurred to give intermediate 17(a,b) followed by acetylation of the NH group to afford the N-(3-cyano-4-(substituted)-4,10-dihydrobenzo[b]pyrano[2,3-e][1,4]thiazin-2-yl)acetamide 18(a,b), according to the method [15]. (Scheme 2). The structure of compounds 15(a,b) and 18(a,b) determined based on the basis of elemental analysis and spectral data. Thus, the IR spectrum of compound 18(a,b) showed disappearance of (CN)group.

3.1.1. CDK inhibiting properties

The anti-CDK activity of the newly synthesized compounds (Table1) was determined using the Millipore Kinase Profiler service [Y. Cheng, W.H. Prusoff, Relationship between inhibition constant (KI) and concentration of inhibitor causing 50 percent inhibition (I50) of the enzymatic reaction, [44]

All newly synthesized compounds selectively inhibited all CDKs in the low nanomolar range and exhibited higher inhibitory activity than flavopiridol. Compounds 3a, 10 (a,b), 9 (a,b), 18b showed higher inhibitory activity against CDK7H and recorded CDK7H.

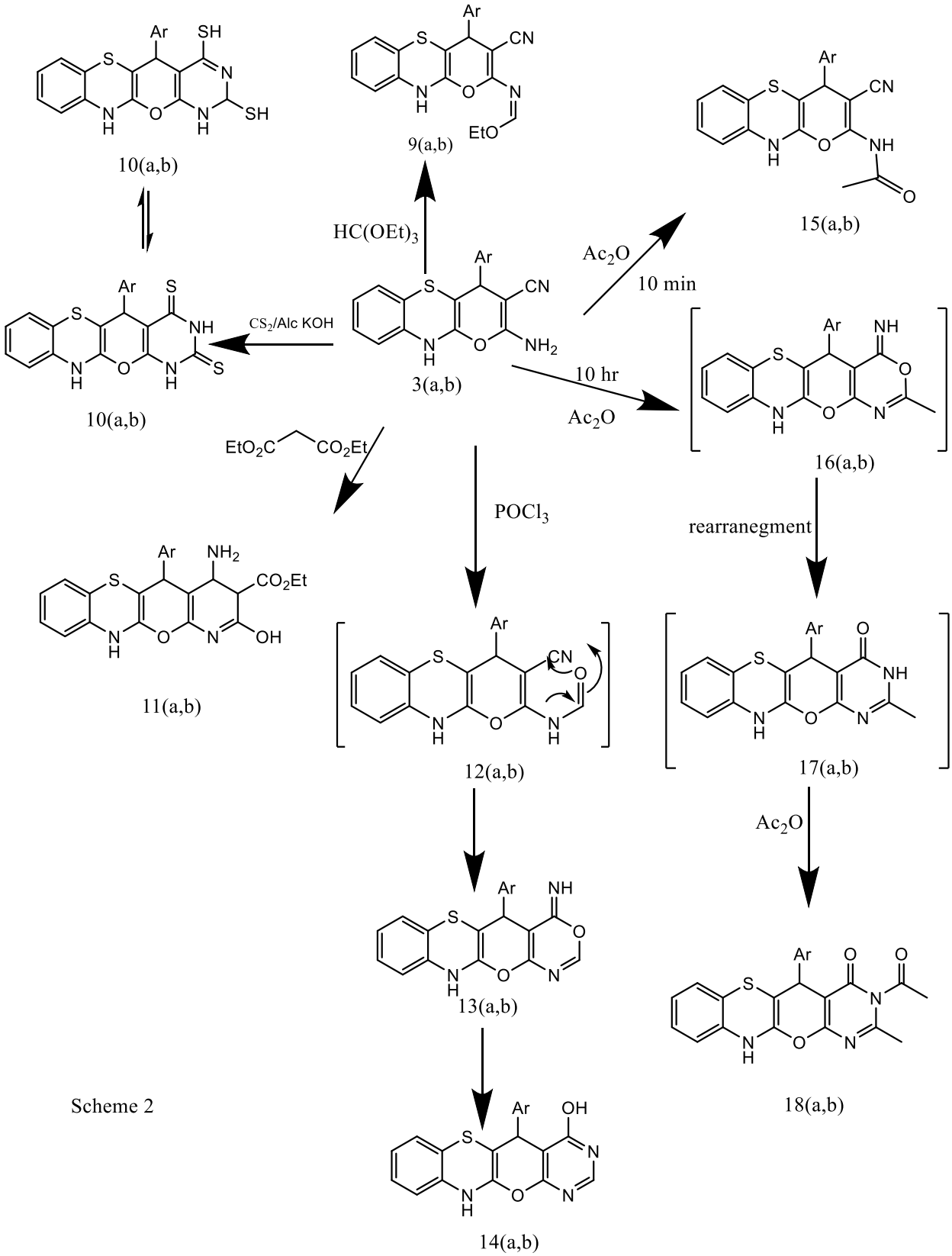
10(a,b)
9(a,b)
15(a,b)
HC(OEt)3
Ac2O
10 min
CS2/Alc KOH
3(a,b)
10 hr
Ac2O
10(a,b)
16(a,b)
EtO2C
CO2Et
POCl3
rearranegment
11(a,b)
12(a,b)
17(a,b)
Ac2O
13(a,b)
18(a,b)
14(a,b)

Scheme 2

Table 1. CDK inhibiting effect of tested compounds

Compound	Kinase inhibition, Ki (nM)				
	CDK9T1	CDK7H	CDK1B	CDK2E	CDK6D3
18b	0.11	0.05	1.11	2.33	0.55
10a	0.12	0.07	1.56	2.67	0.68
10b	0.15	0.09	1.77	3.56	0.78
9a	0.17	1.11	1.89	4.88	0.89
9b	0.21	1,15	2.11	6.18	0.91
3a	0.34	1.22	2.59	9.24	0.92
Flavopiridol	3	113	13	79	265

3.1.2. In vitro anti-VEGFR-2 screening

Studying anti-VEGFR-2 activity of the synthesized compounds (Table 2) showed compound (**3a**) as the most active compound (IC50 = 0.094 nM) and showing even a higher activity than the reference drug (IC50 = 2nM).

Table 2. Anti-VEGFR-2 activity of the synthesized compounds

Compound	Enzymatic inhibition (IC50/nM)
	VEGFR-2
18b	0.055
10a	0.067
10b	0.069
9a	0.071
9b	0.089
3a	0.094
vandetanib	69
Sorafenib	2

3.1.3. In vitro anticancer activity

All target compounds were screened for anticancer activity against various 18 types of human cancer cell lines using the MTT assay by the Mossman method [45]. (Tables 3a and 3b).

Table 3a. In vitro anticancer activity of tested compounds.

Compound	IC50 (nM)								
	Colon carcinoma			Lung carcinoma		Breast carcinoma	Cervical carcinoma	Leukemia	
	HCT116 (p53 wt, Rb)	HCT116 (p53 null, Rb)	HT29	A549	H460	MCF-7 (p53 wt, Rb)	HeLa	HL60	K562
18b	342.56	1345.65	976.43	50.13	138.39	9.44	113.45	4567.	7881.45
10a	4356.45	1456.34	1234.21	62.16	142.56	11.23	114.67	5785.	8777.23
10b	465.56	1789.78	1567.53	78.76	156.78	14.76	115.78	7884.	8994.15
9a	789.76	1873.32	1984.43	88.11	167.65	18.29	122.56	8993.	9467.38
9b	876.76	1923.67	2165.65	92.32	178.78	22.56	134.67	9441.	9887.67
3a	987.54	2111.56	3122.97	94.55	192.13	23.54	144.67	9553.	11244.55

Table 3b In vitro anticancer activity of tested compounds.

Compound	IC50 (µM)								
	Prostate carcinoma			Renal carcinoma		Pancreatic carcinoma	Hepatic carcinoma	Ovarian carcinoma	
	PC3	DU145	LNCaP	CAK1-1 -1	IGROV	Miapaca-2	Hep G2	A2780 -3	SKOV
18b	4.78	5.45	4.65	2.34	8.45	10.45	8.87	11.22	2.23
10a	5.89	6.76	5.45	3.54	9.12	12.38	9.90	12.56	2.34
10b	8.67	7.89	7.36	5.56	12.25	14.65	10.12	15.76	2.65
9a	11.64	8.54	8.26	8.67	16.78	16.43	13.24	17.28	2.78
9b	13.88	9.32	9.57	9.45	18.26	17.78	15.43	19.20	2.81
3a	20.12	10 .45	11.68	9.93	19.88	18.78	16.66	19.50	2.87

3.1.4. Molecular dynamics simulation and target identification

3.1.4.1. Molecular dynamics and system stability

Molecular dynamics simulation was used to predict the performance of the prepared compounds when binding to the active site of the protein, as well as its interaction and stability by simulation [46, 47] . System stability validation is essential to monitor disturbed movements and avoid phenomena that may develop during simulation. This study evaluates the mean square deviation (RMSD) to measure the stability of the system during the simulation of 20 ns. This study evaluates the Root Mean Square Deviation (RMSD), which measures the stability of the system during the simulation of 20 ns. The mean RMSD values recorded for all frameworks of the apo-protein system and the 18b complex system for VEGFR2 were 1.85 Å and 1.62, respectively. (Fig. 1A).

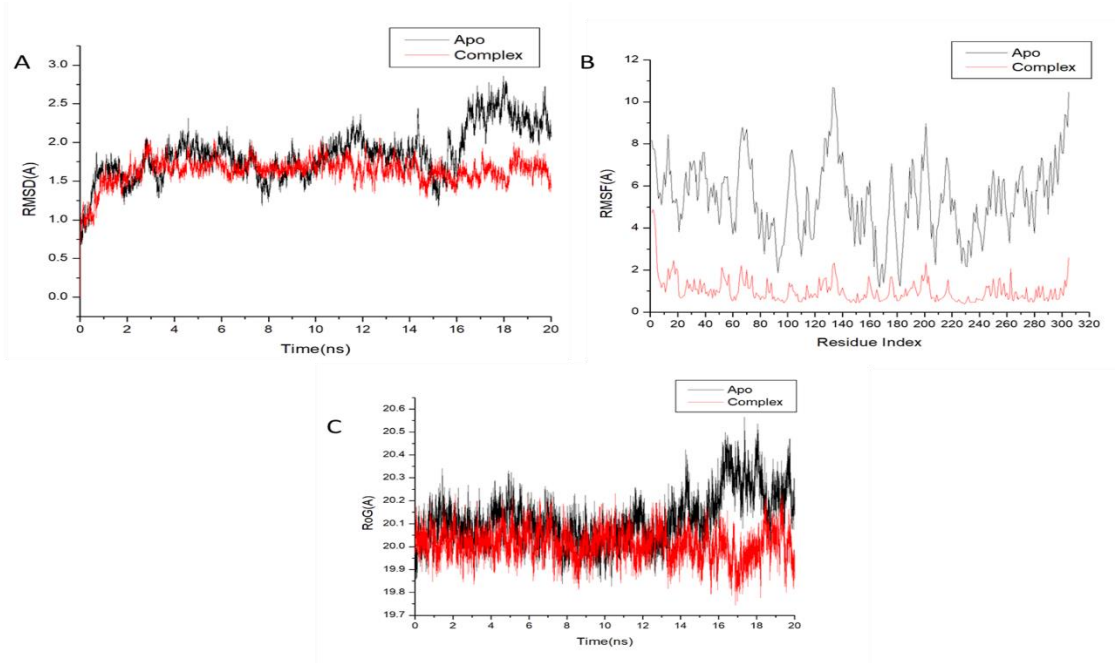

Figure 1: [A] RMSD of Cα atoms of the protein backbone atoms. [B] RMSF of each residue of the protein backbone Cα atoms [c] RoG of Cα atoms of protein residues of the backbone atoms relative (black) to the starting minimized over 20 ns for the VEGFR2s protein with ligand 18b (red).

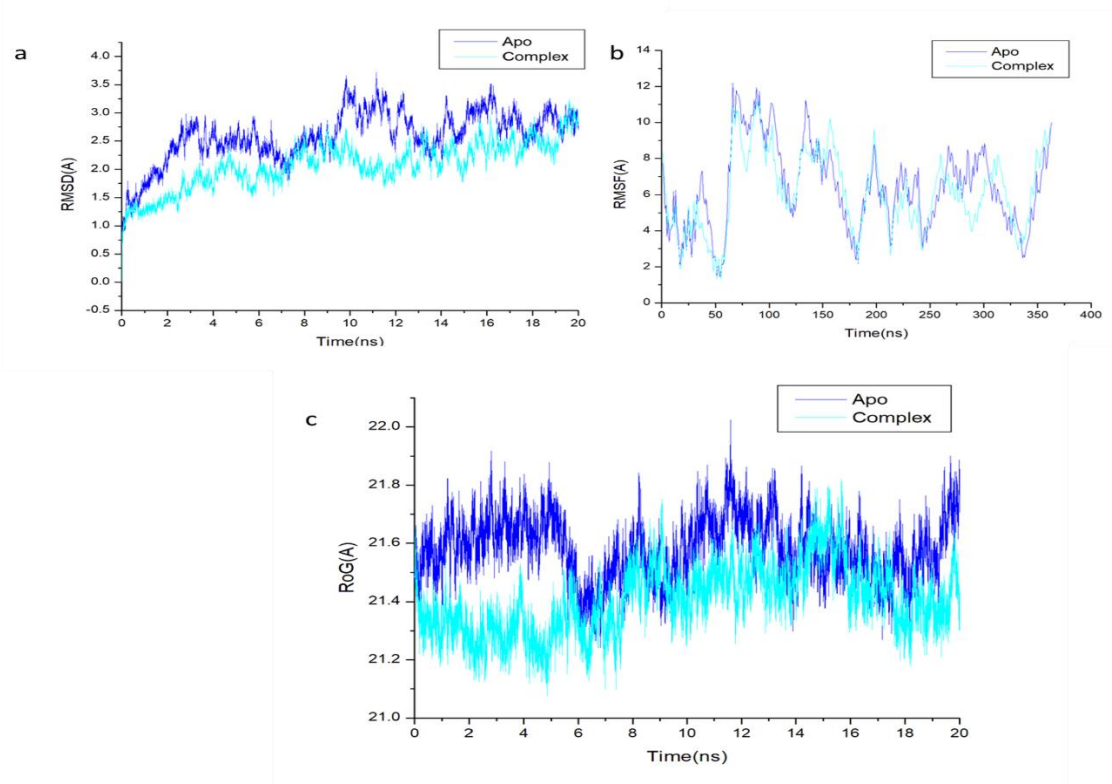

Figure 2: [A] RMSD of Cα atoms of the protein backbone atoms. [B] RMSF of each residue of the protein backbone Cα atoms [c] RoG of Cα atoms of protein residues of the backbone atoms relative (blue) to the starting minimized over 20 ns for the CAK protein with ligand 18b (Cyn).

While the average RMSD values recorded for all the frame works of the apo-protein system and the 18b complex system for CAK were 2.59 Å and 2.07 Å, respectively. (Figure 2a). From these results, we reveal that the protein-bound 18b Complex systems adopt relatively more stable conformations than other systems studied in both targets .It is critical for examining residue behavior and their connection with the ligand to assessing protein structural flexibility upon ligand binding during MD simulation [48] . Using Root-Mean-Square Fluctuation (RMSF) algorithm Protein residues fluctuations evaluated to evaluate the effect of inhibitor binding aganist the respective targets above 20 ns simulations. Computed average RMSF values were 5.39Å, and 1.02 Å for apo-protein, and 14b-complex system for the VEGFR2s , respectively. While, The computed average RMSF values were 6.41Å, and 6.14 Å for apo-protein, and 18b-complex system for the CAK , respectively . In general residue fluctuations of individual systems are represented in Figure 1B, and 2b. Values revealed that the lower residue fluctuation than the other systems on both targets was 18b -bound to protein complex system

The radius of gyration (Rg) is an indicator of protein structure rigor as well as stability during simulation. As shown in Figure 1C, the Rg values of apo-protein and complex with compound 18b are 20.11 Å and 19.88 Å for VEGFR2. While the Rg values of apo-protein and complex with compound 18b were 21.58 Å and 21.40 Å for CAK (Figure 2c). The Rg of the ligand-binding protein was found to have a stiffer structure than that of the Apo protein.

3.1.5. Binding interaction mechanism based on binding free energy calculation:

To determine the free binding energies of small molecules to biological macromolecules, the molecular mechanical energy technique (MM/GBSA) is a popular method, incorporating the general resolution of continuous generation and surface, and may be more reliable than the score [49]. To calculate the bound free energy by extracting the orbital snapshot of the system, the program MM-GBSA in AMBER18 was used. In (Table 4), all reported calculated energy components (except ΔGsolv) have high negative values indicating favorable interactions. These results indicate that the binding affinity of 18b binding to VEGFR2 and CAK is -31.48 kcal/mol, -37.08 kcal/mol, respectively.

ΔEele = electrostatic energy; ΔEvdW = van der Waals energy;ΔGsolv = solvation free energy; ΔGbind = calculated total binding free energy.

The interaction between 18b and protein receptor residues VEGFR2 and CAK is driven by more active vander Waals energy components, as demonstrated by a detailed examination of each individual energy contribution, resulting in free energy. Reported link. (Table 4).

Table 4: The calculated energy binding for the 18b compounds against the VEGFR2s, and CAK protein receptors.

Energy Components (kcal/mol)					
Complex	**ΔE_{vdW}**	**ΔE_{elec}**	**ΔG_{gas}**	**ΔG_{solv}**	**ΔG_{bind}**
18b- VEGFR2s	-47.23 ± 0.40	-1.78± 0.49	-49.01± 0.54	17.53± 0.32	-31.48± 0.43
18b-CAK	-45.06±0.52	-23.59±1.10	-68.66±1.13	31.57±1.10	-37.08±0.46

ΔEvdW = van der Waals energy; ΔEele = electrostatic energy; ΔGsolv = solvation free energy; ΔGbind = calculated total binding free energy

3.1.6. Identification of the critical residues responsible for ligands binding:

The total energy involved when 14b binds to these enzymes can be broken down into the involvement of individual site residues to gain more knowledge about the key residues involved in the inhibition of VEGFR2 receptors. Connection of CAK receptor 18b to is observed mainly from residues Ala 75 (-0.161 kcal/mol), Leu 76 (-0.389 kcal/mol), Ser 78 (-0.368 kcal/mol), Glu 79 (-1.133 kcal/mol). , Leu 80 (-0.253

kcal/mol), Ile 82 (-1.765 kcal/mol), Leu 83 (-2.80 kcal/mol), Ile 86 (-0.787 kcal/mol), Val 92 (-0.437 kcal/mol) mol), Val 93 (-0.402 kcal/mol), Val 108 (-0.651 kcal/mol), Val 110 (-0.793 kcal/mol), Leu 156 (-0.502 kcal/mol), Cys 182 (-2.086 kcal/mol) mol) mol) mol) , Asp 183 (-0.329 kcal/mol), Phe 184 (-0.509 kcal/mol). On the other hand, the major beneficial contributions of 18b compounds to the CAK receptor are mainly at residues Leu 74 (-0.876 kcal/mol), Gly 75 (-1.33 kcal/mol) and Glu 76 (-0.325 kcal/mol). It has been constructed. mol), Ala 80 (-0.6 kcal/mol), Val 82 (-2.71 kcal/mol), Ala 95 (-0.614 kcal/mol), Lys 97 (-1.471 kcal/mol), Glu 113 (-0.406 kcal/ mol) mol), Phe 112 (-0.919 kcal/mol), Met 145 (-1.126 kcal/mol), Thr 147 (-0.284 kcal/mol), Asn193 (-0.24 kcal/mol), Leu 194 (-0.219 kcal /mol)), Leu 195 (-2.104 kcal/mol), Ala 205 (-2.22 kcal/mol), Asp 206 (-1.119 kcal/mol).

4. Conclusion

In summary, The purpose of the present work is the synthesis of new Pyrano[2,3-e][1,4]thiazine derivatives, which are projected to show potent anticancer activity. Thus, the parent Pyrano[2,3-e][1,4]thiazine derivatives 3(a,b) was subjected to a series of various reactions to get the target compounds. In vitro cytotoxic evaluation of all the novel Pyrano[2,3-e][1,4]thiazine derivatives against human cancer cell. Compounds 3a, 10(a,b), 9(a,b), 18b showed higher inhibitory activity against CDK7H and recorded CDK7H. Studying anti-VEGFR-2 activity showed that compound (**3a**) as the most active compound (IC50 = 0.094 nM) and showing even a higher activity than the reference drug (IC50 = 2nM).

5. Conflict of interests:

The authors declare that they have no conflict of interest

6. References

1. Green, G.R., *Pyrans and their benzo derivatives synthesis," in Comprehensive Heterocyclic Chemistry II.* Pergamon Press, Oxford, UK 1995: p. 469.
2. Abdelrazek, F.M., et al., *Synthesis and molluscicidal activity of new chromene and pyrano [2, 3-c] pyrazole derivatives.* Archiv der Pharmazie: An International Journal Pharmaceutical and Medicinal Chemistry, 2007. **340**(10): p. 543-548.
3. Bonsignore, L., et al., *Synthesis and pharmacological activity of 2-oxo-(2H) 1-benzopyran-3-carboxamide derivatives.* European Journal of Medicinal Chemistry, 1993. **28**(6): p. 517-520.
4. Witte, E., P. Neubert, and A. Roesch, *7-(Piperazinylpropoxy)-2H-1-benzopyran-2-ones.* Ger Offen DE, 1986. **3427985**.
5. Lei, M., L. Ma, and L. Hu, *A green, efficient, and rapid procedure for the synthesis of 2-amino-3-cyano-1, 4, 5, 6-tetrahydropyrano [3, 2-c] quinolin-5-one derivatives catalyzed by ammonium acetate.* Tetrahedron Letters, 2011. **52**(20): p. 2597-2600.
6. Harb, A.F.A., et al., *Notizen/notes polyazanaphthalenes, I the reaction of ethyl 6-amino-5-cyano-4-aryl-2-methyl-4H-pyran-3-carboxylate with nucleophilic reagents.* Liebigs Annalen der Chemie, 1989. **1989**(6): p. 585-588.
7. Quintela, J., C. Peinador, and M.J. Moreira, *A novel synthesis of pyrano [2, 3-d] pyrimidine derivatives.* Tetrahedron, 1995. **51**(20): p. 5901-5912.
8. Srivastava, S., S. Batra, and A. Bhaduri, *A Facile Acid Catalyzed Ring Transformation of 4H-Pyrans to 1, 2, 3, 4-Tetrahydropyridin-2-ones and 3, 4-Dihydronaphtho (1, 2-b) pyran-2 (H)-ones.* ChemInform, 1996. **27**(34): p. no-no.
9. Gupta, S., *Quantitative structure-activity relationship studies on anticancer drugs.* Chemical reviews, 1994. **94**(6): p. 1507-1551.
10. Jemal, A., et al., *Global cancer statistics.* CA: a cancer journal for clinicians, 2011. **61**(2): p. 69-90.
11. Cohen, P., *The role of protein phosphorylation in human health and disease. The Sir Hans Krebs Medal Lecture.* European journal of biochemistry, 2001. **268**(19): p. 5001-5010.
12. Traxler, P., et al., *Tyrosine kinase inhibitors: from rational design to clinical trials.* Medicinal research reviews, 2001. **21**(6): p. 499-512.
13. Zwick, E., J. Bange, and A. Ullrich, *Receptor tyrosine kinases as targets for anticancer drugs.* Trends in molecular medicine, 2002. **8**(1): p. 17-23.
14. Sarabipour, S., K. Ballmer-Hofer, and K. Hristova, *VEGFR-2 conformational switch in response to ligand binding.* Elife, 2016. **5**.

15. Abhinand, C.S., et al., *VEGF-A/VEGFR2 signaling network in endothelial cells relevant to angiogenesis.* Journal of cell communication and signaling, 2016. **10**(4): p. 347-354.
16. Hicklin, D.J. and L.M. Ellis, *Role of the vascular endothelial growth factor pathway in tumor growth and angiogenesis.* Journal of clinical oncology, 2005. **23**(5): p. 1011-1027.
17. Guo, S., et al., *Vascular endothelial growth factor receptor-2 in breast cancer.* Biochimica et Biophysica Acta (BBA)-Reviews on Cancer, 2010. **1806**(1): p. 108-121.
18. Yamaguchi, R., et al., *Expression of vascular endothelial growth factor in human hepatocellular carcinoma.* Hepatology, 1998. **28**(1): p. 68-77.
19. Yan, J.-D., et al., *Expression and prognostic significance of VEGFR-2 in breast cancer.* Pathology-Research and Practice, 2015. **211**(7): p. 539-543.
20. Folkman, J., *Angiogenesis: an organizing principle for drug discovery?* Nature reviews Drug discovery, 2007. **6**(4): p. 273-286.
21. Madkour, H.M., et al., *Antioxidant Activity of Novel Pyrimidines Derived from Arylidenes.* International Journal of Pharmaceutical Science and Health Care, 2014. **4**(2): p. 102-115.
22. Abdel-Latif, E., et al., *Synthesis and antitumor activity of some new pyrazolo [3, 4-d] pyrimidine and pyrazolo [3, 4-b] pyridine derivatives.* Egyptian Journal of Basic and Applied Sciences, 2016. **3**(1): p. 118-124.
23. Makki, M.S., et al., *Designing and synthesis of new fluorine substituted pyrimidine-thion-5-carbonitriles and the related derivatives as photochemical probe agents for inhibition of vitiligo disease.* 2012.
24. Salaheldin, A.M., A.M. Oliveira-Campos, and L.M. Rodrigues, *Heterocyclic synthesis with nitriles: synthesis of pyrazolopyrimidine and pyrazolopyridine derivatives.* Synthetic Communications®, 2009. **39**(7): p. 1186-1195.
25. Ghorab, M.M., et al., *Anticancer and radiosensitizing evaluation of novel sulfonamides with quinoline and pyrimidoquinoline groups.* Research on Chemical Intermediates, 2015. **41**(2): p. 647-661.
26. Xi, L., et al., *Novel 5-anilinoquinazoline-8-nitro derivatives as inhibitors of VEGFR-2 tyrosine kinase: synthesis, biological evaluation and molecular docking*. Organic & Biomolecular Chemistry, 2013. **11**(26): p. 4367-4378.
27. Greber, B.J., et al., *The cryoelectron microscopy structure of the human CDK-activating kinase.* Proceedings of the National Academy of Sciences, 2020. **117**(37): p. 22849-22857.
28. McTigue, M., et al., *Molecular conformations, interactions, and properties associated with drug efficiency and clinical performance among VEGFR TK inhibitors.* Proceedings of the National Academy of Sciences, 2012. **109**(45): p. 18281-18289.
29. Pettersen, E.F., et al., *UCSF Chimera—a visualization system for exploratory research and analysis.* Journal of computational chemistry, 2004. **25**(13): p. 1605-1612.
30. Li, H., A.D. Robertson, and J.H. Jensen, *Very fast empirical prediction and rationalization of protein pKa values.* Proteins: Structure, Function, and Bioinformatics, 2005. **61**(4): p. 704-721.
31. Halford, B., *Reflections on CHEMDRAW.* Chemical & Engineering News, 2014. **92**(33): p. 26-27.
32. Hospital, A., et al., *Molecular dynamics simulations: advances and applications.* Advances and applications in bioinformatics and chemistry: AABC, 2015. **8**: p. 37.
33. Lee, T.-S., et al., *GPU-accelerated molecular dynamics and free energy methods in Amber18: performance enhancements and new features.* Journal of chemical information and modeling, 2018. **58**(10): p. 2043-2050.
34. Wang, J., et al., *Automatic atom type and bond type perception in molecular mechanical calculations.* Journal of molecular graphics and modelling, 2006. **25**(2): p. 247-260.
35. Berendsen, H.J., et al., *Molecular dynamics with coupling to an external bath.* The Journal of chemical physics, 1984. **81**(8): p. 3684-3690.
36. Roe, D.R. and T.E. Cheatham III, *PTRAJ and CPPTRAJ: software for processing and analysis of molecular dynamics trajectory data.* Journal of chemical theory and computation, 2013. **9**(7): p. 3084-3095.
37. Seifert, E., *OriginPro 9.1: scientific data analysis and graphing software-software review.* Journal of Chemical Information and Modeling, 2014. **54**(5): p. 1552.
38. Kollman, P.A., et al., *Calculating structures and free energies of complex molecules:*

combining molecular mechanics and continuum models. Accounts of chemical research, 2000. **33**(12): p. 889-897.
39. Ylilauri, M. and O.T. Pentikäinen, *MMGBSA as a tool to understand the binding affinities of filamin–peptide interactions.* Journal of chemical information and modeling, 2013. **53**(10): p. 2626-2633.
40. Hayes, J.M. and G. Archontis, *MM-GB (PB) SA calculations of protein-ligand binding free energies.* Molecular dynamics-studies of synthetic and biological macromolecules, 2012: p. 171-190.
41. Hou, T., et al., *Assessing the performance of the MM/PBSA and MM/GBSA methods. 1. The accuracy of binding free energy calculations based on molecular dynamics simulations.* Journal of chemical information and modeling, 2011. **51**(1): p. 69-82.
42. Greenidge, P.A., et al., *MM/GBSA binding energy prediction on the PDBbind data set: successes, failures, and directions for further improvement.* Journal of chemical information and modeling, 2013. **53**(1): p. 201-209.
43. Sitkoff, D., K.A. Sharp, and B. Honig, *Accurate calculation of hydration free energies using macroscopic solvent models.* The Journal of Physical Chemistry, 1994. **98**(7): p. 1978-1988.
44. Cheng, Y.-C., *Relationship between the inhibition constant (Ki) and the concentration of inhibition, which causes 50% inhibition (IC_< 50>) of an enzymatic reaction.* Biochem Pharmacol., 1973. **22**: p. 3099-3108.
45. Mosmann, T., *Raptid colorimetric assay for cellular growth and survival: application to proliferation and cytotoxicity assays.* Journal of immunological methods, 1983. **65**(1-2): p. 55-63.
46. Hasanin, M., et al., *Synthesis of novel heterocyclic compounds based on dialdehyde cellulose: characterization, antimicrobial, antitumor activity, molecular dynamics simulation and target identification.* Cellulose, 2021. **28**(13): p. 8355-8374.
47. Mirzaei, S., et al., *Design, synthesis and biological evaluation of novel 5, 6, 7-trimethoxy-N-aryl-2-styrylquinolin-4-amines as potential anticancer agents and tubulin polymerization inhibitors.* Bioorganic Chemistry, 2020. **98**: p. 103711.
48. Machaba, K.E., N.N. Mhlongo, and M.E. Soliman, *Induced mutation proves a potential target for TB therapy: a molecular dynamics study on LprG.* Cell Biochemistry and Biophysics, 2018. **76**(3): p. 345-356.
49. Cournia, Z., B. Allen, and W. Sherman, *Relative binding free energy calculations in drug discovery: recent advances and practical considerations.* Journal of chemical information and modeling, 2017. **57**(12): p. 2911-2937.